Modeling the Cavitation Free Energy

Franca Maria Floris*

Dipartimento di Chimica e Chimica Industriale, Università di Pisa, Via Risorgimento 35, 56126 Pisa, Italy

Received: June 25, 2005; In Final Form: September 16, 2005

A new expression to compute the cavitation free energy has been derived by integrating a new model to fit its derivative with respect to the cavity radius. The derivatives were obtained from Monte Carlo simulations data of the contact values of distribution functions for hard-sphere solutes in TIP4P water at 298 K and 1 atm. The new expression, formulated in the framework of the thermodynamics of surfaces and unlike the classical simple models, gives good results also for very small cavities with a radius of ∼1 Å. The contribution to the free energy of a term, which depends on the excess number of molecules at the dividing surface, has been taken into account and discussed for the assumed dependence on r of the surface tension. The asymptotic behavior of the derivative has thus been considered, and a function $t(r)$, which is 0 at $r = 0$ and 1 at infinity, has been introduced to describe the transition from small to large length regimes. The value of the surface tension obtained by fitting is in very good agreement with that obtained from a simulation of the liquid/vapor interface by using the TIP4P model.

1. Introduction

The cavitation free energy is a contribution to the solvation free energy. It is of basic importance in the usual partition that is based on the different nature of solute−solvent interactions. In particular, it has been studied in hydrophobic solutes as is widely documented in the literature (see, for example, refs 1−5 and references therein).

Although by use of computer simulations[6−17] this term can be calculated directly for an assumed solute−solvent repulsive potential, such simulations are still too long for routine calculations of the solvation free energy. Statistical theories[18,19] would seem to offer a valid alternative, and models based on the scaled particle theory (SPT)[20−22] or on the thermodynamics of surfaces[23] are more appealing in terms of simplicity. This is why it is usually preferable to combine them with polarizable continuum models.[23,24] Since these methods neglect the solvent structure around the solute, some ad hoc parametrizations are required in these applications. Practical recipes obtained by comparing computed values of solvation free energies are commonly employed. However, extracting cavitation free energies from experimental data requires some particular care, as recently pointed out by Amovilli and Floris.[25] Moreover, the choice of the model used to compute this term together with the parametrization approach are very delicate points. So, it is not surprising that different parametrization approaches can lead to discrepancies in the parameter values as recently shown.[26] On the other hand, a test of simple models by comparison with simulation or statistical theory results should prevent the risk of misinterpretations due to the superposition of effects arising from different approximations.

What appears to be more difficult is finding a simple model that is valid at different length scales, from small to large cavities. The different hydration mechanisms observed in the two scales are now of great interest.[16,17,19,27−29] At ambient conditions, Huang et al.[16] have found that the crossover to a large length scale regime occurs near 10 Å for hard-sphere solutes in SPC/E[30] water. In our previous work,[27] this size has also been found to determine a change in the sign of the nonideal contribution to the excess volume of such solutes. The predicted positive sign of this quantity for cavities with a radius larger than ∼9 Å appears to be a direct consequence of the depletion of solvent molecules at the interface that starts in this region. A comparison of this quantity with simulation results showed the failure of the simple model based on SPT[20] for cavities with contact radius larger than 4 Å. Bad performances in the same region were also highlighted by the BMCSL equation developed on the basis of a theory of mixtures of hard spheres proposed by Boublik[31] and Mansoori et al.[32]

According to other simple models, which share the reference to the thermodynamics of surfaces,[33−39] the cavitation free energy of a macroscopic cavity scales with its surface. Such models usually introduce a curvature correction to the limiting value of the surface tension for a planar interface. This kind of model derived from Tolman's expression[40] appears to be suitable for a macroscopic spherical cavity. For a contact radius in a range between 6 and 10 Å, Huang et al.[16] fitted their simulation results with this simple model. For smaller cavities with contact radii approaching the molecular radius of the solvent, other terms need to be added. For example, adding a constant might be enough to have acceptable values of cavitation free energies. Simulation results of cavitation free energy are reproduced by this model within ∼5% for contact radii between 1 and 5 Å.[15] This model is also in agreement with the approximate expression derived from the SPT[20] by Taylor's expansion around a contact radius corresponding to a point solute.

The convergence to substantially the same expression but this time starting from the opposite scale regime is very interesting.[21] This view is supported by the reasonable values of surface tension generally obtained[15,21] by interpreting the SPT approximate expression in terms of the thermodynamics of surfaces. Nevertheless, limits of this expression have been found when it is used to derive other properties in both scale regimes. With regard to the inadequacy in the large scale regime, see ref 27. In the small scale regime, the failure in predicting the contact

* E-mail: floris@dcci.unipi.it.

10.1021/jp053457+ CCC: $30.25
Published on Web 11/30/2005

values of the solute−solvent radial distribution function (rdf) has been noted.[41,42] For contact radii larger than ∼1.7 Å, improvements have been obtained[15,42,43] by adding another term to the correction factor of the surface tension.[41] Finally, there is a model even more simple than all those cited above that scales the cavitation free energy with the cavity surface, since a different dividing surface is chosen. Despite its simplicity, this model has performed well in reproducing cavitation free energies from simulations in the small scale regime.[15,44]

In this work, a new simple model is proposed to fit the derivative of the cavitation free energy obtained from simulation data of contact values of radial distribution functions for hard-sphere cavities in TIP4P water. The model refers to a dividing surface located at the contact radii between the cavity and the oxygen centers. As a further test of the model, cavitation free energies computed by integration are compared to results obtained by using information theory.[2,4,45−48]

The paper is organized as follows. Section 2 gives a brief review of the simple models whose expressions have been used to fit the data. Section 3 presents the new model proposed to fit the derivative, which by integration leads to a new expression for the cavitation free energy. Section 4 shows the performance of this model and also a comparison with some commonly used simple models.

2. Simple Models

A simple model that is frequently used in fitting simulation results of cavitation free energies (W) is the one derived from the thermodynamics of surfaces,[40] namely,

$$W(r) = P\Delta V + 4\pi\tilde{\gamma}\left(1 - 2\frac{\tilde{\delta}}{r}\right)r^2 \qquad (1)$$

where $\tilde{\gamma}$ and $\tilde{\delta}$ have the dimension of a surface tension and a length, respectively. The latter is a curvature parameter, r being the contact radius. The dividing surface is thus the accessible surface, which in principle is not coincident with the surface of tension. In the latter case, $\tilde{\delta}$ is the Tolman length, that is, the distance between the equimolar surface and the surface of tension. In the limit of infinite radius, eq 1 reduces to the expression of the work needed to increase the area of a planar interface. However, for very small cavities, the same equation does not give the correct behavior of contact values of solute−solvent radial distribution functions. As already pointed out,[9] a comparison with the contact values of solute−solvent distribution, $G(r)$, is a stringent test of a model for the calculation of W. These contact values are related to W by

$$G(r) = \frac{1}{4\pi r^2 \rho_0 k_B T}\frac{dW}{dr} \qquad (2)$$

where k_B is the Boltzmann constant, T is the temperature, and ρ_0 is the solvent density.

According to Stillinger's functional form for $G(r)$, an improvement of the model consists of adding a term proportional to $1/r^3$ in the surface tension correction factor. Moreover, a constant can be added to eq 1 without changing $G(r)$. This entails adding a term proportional to $1/r^2$ in the correction factor of $\tilde{\gamma}$, as written in the following expression

$$W(r) = P\Delta V + 4\pi\tilde{\gamma}\left[1 - 2\frac{\tilde{\delta}}{r} + \frac{w_0}{4\pi\tilde{\gamma}r^2} - \frac{\alpha}{r^3}\right]r^2 \qquad (3)$$

In the context of the thermodynamics of surfaces, $w_0/(4\pi\gamma r^2)$ and α/r^3can be seen as higher terms in the expansion of the approximate expression derived by Tolman.[40] Despite the initial doubts[39,40] about the physical meaning of these terms, there has recently been some interest[49] in the computation of the constants associated with the Gaussian curvature ($1/r^2$).[50] Note that, for $\alpha = 0$, the expression above is equivalent to the SPT model,[15,20,21] where $\tilde{\gamma}$, $\tilde{\delta}$ and w_0 are written in terms of the molecular size of the liquid, which is the only parameter of the model. Both the SPT model and eq 3 have shown some inadequacy due to the lack of important terms in going from microscopic to macroscopic cavities.

However, SPT gives exact expressions that in practical applications can be used up to a radius such that no triplets of solvent centers can be found inside of the cavity. Namely, for the free energy

$$W(r) = -k_B T \ln\left[1 - \langle n\rangle + \frac{1}{2}\langle n(n-1)\rangle\right] \qquad (4)$$

where n is the instantaneous number of centers within the cavity of radius r. According to eq 4, in water for the contact values of cavity−oxygen rdf's, SPT[20] gives

$$G_{SPT}(r) = \frac{1 + (\pi\rho_0/r)\int_0^{2r} ds\, g_{OO}(s)(s^3 - 2rs^2)}{1 - \rho_0\left(\frac{4}{3}\pi r^3\right) + (\pi\rho_0)^2\int_0^{2r} ds\, g_{OO}(s)(s^5/6 - 2r^2s^3 + 8r^3s^2/3)} \qquad (5)$$

where g_{OO} is the O−O rdf in pure water. For oxygens in liquid water at ambient conditions, these expressions can be successfully used up to a radius ∼1.9 Å. The requirement of continuity at some specified radius for $G(r)$ and its derivative gives an alternative to the fitting procedure for the determination of $\tilde{\delta}$ and α, as already proposed and used in the literature.[41−43]

Note once again that here r is the solute−solvent contact distance. This is the most usual and natural choice for a dividing surface when working with hard spheres. In this case, we need to introduce in eqs 1 and 3 a term proportional to n_s, the excess number of molecules at the surface.[36] This excess property depends on the local structure of the system at the interface and on the macroscopic densities of the regions separated by the interface. A particular choice for the dividing surface is the equimolar surface, for which $n_s = 0$. Any other arbitrary choice for the dividing surface entails introducing the free energy contribution $\tilde{\mu}_s n_s$, $\tilde{\mu}_s$ being a chemical potential. The presence of this term can be seen as a sort of correction to the unrealistic view in which the dividing surface abruptly separates two bulk regions of homogeneous densities. How this term is actually computed will be the subject of a future paper, while here we limit ourselves to taking it into account when deriving and discussing the new proposed model.

3. Beyond the Usual Simple Model

3.1. A Model from the Macroscopic Limit. For an arbitrary choice of the dividing surface, such as the one defined by the contact radii of hard-sphere solutes, a rigorous treatment of curved surfaces based on the thermodynamics of surfaces gives quite a complex expression.[34] Since this expression is limited to large cavities, here we prefer to follow a reasonable route, which only takes into account the main ideas of Gibbs formulation. With P and T constant, for the cavitation free energy, we start with the following expression:

$$W(r) = 4\pi\gamma f_c(r) r^2 + \tilde{\mu}_s(r) n_s(r) + P\Delta V \qquad (6)$$

where γ is the surface tension in the limit of a planar interface, $f_c(r)$ is a function describing curvature corrections, $\tilde{\mu}_s$ is a chemical potential, and $n_s(r)$ is the excess number of molecules at the chosen dividing surface. In the last term, ΔV is the variation of volume due to the insertion of the cavity in the liquid. Performing the derivative with respect to the radius, we obtain

$$\frac{dW}{dr} = 4\pi\gamma[f_c'(r)r + 2f_c(r)]r + \tilde{\mu}_s'(r)n_s(r) + \tilde{\mu}_s(r)n_s'(r) + P\frac{d\Delta V}{dr} \quad (7)$$

In eqs 6 and 7, $\tilde{\mu}_s$ shows dependence on r apparently in contrast with chemical equilibrium conditions. According to thermodynamics, such dependence is possible only in the presence of an external field, which in this case could be that due to the solute. At infinite dilution, the Gibbs−Duhem equation suggests that the chemical potential of the solvent molecules is only slightly changed with respect to that in the pure liquid.[51] Nevertheless, we retain that at least in principle $\tilde{\mu}_s$ could depend on r for the following reasons: (1) this chemical potential refers to the excess molecules at the dividing surface; (2) the dividing surface is placed in an inhomogeneous region; (3) the dividing surface cannot be coincident with that of the surface tension; (4) the particular dividing surface placed at the contact hard-sphere radius is not a free surface, that is, it can be crossed only in one direction. Hill[34] remarked that all the intensive variables depend on the curvature and that inhomogeneity in particular in small curved surfaces needs quasi-thermodynamic treatments. Local intensive thermodynamic properties were defined in the context of quasi-thermodynamics.[34,38,52] These produced some "bizarre" results on local pressure,[38,52] but the local chemical potential seems well defined and constant everywhere at equilibrium conditions.[52] Although this is not specifically addressed to the points enumerated above, it can be accepted without changing eqs 6 and 7. In fact in these equations, we have used a simpler notation because the dividing surface is placed at the accessible surface, which is connected to the specific physical characteristics of the system. For each case studied, a cavity of radius r has been introduced in liquid water by imposing specific constraints, which can be seen as the effect of a specific external field.[53] We believe that this is sufficient to justify the dependence of $\tilde{\mu}_s$ on r shown explicitly in eqs 6 and 7. In the limit of a very large cavity, we assume that $\tilde{\mu}_s$ is constant but not necessarily the chemical potential of the pure solvent. In the same limit, because the profile of the density distribution tends to a limiting behavior, we expect that the superficial density of the excess number of molecules at the dividing surface will be constant so that $n_s \approx r^2$. An estimate based on typical density profiles for a liquid−gas interface has shown that at very large radii n_s behaves as a quadratic function of r with negative coefficients in agreement with positive nonideal contributions to the molar volume.[27] Thus, at large radii the term in eq 6 that depends on n_s behaves in the same way as the surface contribution to the free energy. Because f_c tends to 1 at infinite radius, the derivative should behave as

$$\lim_{r\to\infty}\frac{dW}{dr} \approx 4\pi Pr^2 + 8\pi\tilde{\gamma}r - 8\pi\tilde{\gamma}\tilde{\delta} + o\left(\frac{1}{r}\right) \quad (8)$$

where $\tilde{\delta}$ has the dimension of a length. Note that in eq 8 we use for the surface tension the symbol $\tilde{\gamma}$ instead of γ to stress that the second term in eq 6 and the nonideal contribution to ΔV give some contribution to $\tilde{\gamma}$ and $\tilde{\delta}$. As in eq 1 also here $\tilde{\gamma}$ and $\tilde{\delta}$ are treated as parameters. Note that the next term of the expansion in eq 8 would be of the order $1/r$, which leads to a logarithmic term in the expression of W. Stillinger, and Cotter[54] excluded the presence of such kinds of contributions on the basis of the analysis of the expansion of the distribution function in the large size limit. Even Tolman's approximate expansion of $\gamma(r)$, which holds in the same limit, excludes the presence of a logarithmic term in the free energy. Moreover, Tully-Smith and Reiss came to the same conclusion on the basis of exact relationships derived for $G(r)$. Nevertheless, very recently the presence of the logarithmic term has been recognized to take a role in wetting−drying at a hard spherical cavity when conditions are very close to liquid−gas coexistence.[55,56] It is out of our scope to enter such a debate, and in the following, we limit our attention to the development of a practical procedure to model the derivative of W with respect to the radius of the cavity. On the basis of this point, we propose the expression

$$\frac{dW}{dr} = 8\pi\tilde{\gamma}t(r)[r - \tilde{\delta}\zeta(r)] + 4\pi Pr^2 \quad (9)$$

where $t(r)$ is a function that describes the transition from small to large scale regimes and $\zeta(r)$ is a scaling function depending on r that corrects $\tilde{\delta}$ in the short length scale. Thus, the validity of eq 9 is extended to a wider range of radii including relatively small cavities. Note that in eq 9, we assumed $\Delta V = {}^4/_3\pi r^3$; thus the term that is proportional to $t(r)$ also includes the correction due to the nonideal volume.[27] Note also that without the scaling of $\tilde{\delta}$, $t(r)$ diverges at $r = \tilde{\delta}$ and would require a larger number of parameters for a good description. We have found that with an appropriate scaling of $\tilde{\delta}$, $t(r)$ behaves as a function that is 0 at $r = 0$ and 1 at infinity. A simple function that can be used for this purpose is

$$\zeta(r) = e^{-\tilde{\delta}_1/r} \quad (10)$$

where $\tilde{\delta}_1$ is a new parameter. Note that a Taylor expansion of $\zeta(r)$ contains a term $\sim 1/r$, which will lead to the debated logarithmic term in the free energy discussed above. We remark that $\zeta(r)$ has been introduced only on the basis of a practical convenience.

A rigorous decomposition of W and its derivative with respect to r as shown in eqs 6 and 7 is not possible without the knowledge of $\tilde{\mu}_s$, n_s, and $f_c(r)$. The assumption of $f_c(r)$ like that given explicitly in eq 1 seems quite reasonable on the basis of previous fitting results. In fact, the same formal dependence on curvature can be assumed, at least in the macroscopic limit, for the two most important dividing surfaces, namely, the equimolar surface and the surface of tension.[36] Therefore, this would hold also for the accessible surface, which is presumably close to these two, and the value of γ should be practically independent from the precise location of the dividing surface.[36,39] This γ should be the measured value of surface tension, which refers to the surface of tension. However, $\tilde{\gamma} \geq \gamma$ and $\tilde{\delta} \leq \delta$ because of the contribution due to the term $\tilde{\mu}_s n_s$ at infinity. The effect may be unimportant in comparison to the uncertainties of the measures and the neglect of this contribution could be reasonable. Only in this case we can use $\tilde{\gamma}$ and $\tilde{\delta}$ to define W_s and the corresponding derivative. Otherwise, we can discuss the quantities

$$\tilde{W}_s = W_s + \lim_{r\to\infty}\tilde{\mu}n_s + P\lim_{r\to\infty}\Delta V_{ni} \quad (11)$$

and the complementary term

$$\tilde{W}_{\tilde{\mu}_s n_s} = W_{\tilde{\mu}_s n_s} + P\Delta V_{ni} - \lim_{r\to\infty} \tilde{\mu}_s n_s - P \lim_{r\to\infty} \Delta V_{ni} \quad (12)$$

where ΔV_{ni} is the nonideal contribution to ΔV.[27] According to the assumptions made above the corresponding derivatives with respect to r are

$$\frac{d\tilde{W}_s}{dr} = 8\pi\tilde{\gamma}(r - \tilde{\delta}) \quad (13)$$

$$\frac{d\tilde{W}_{\tilde{\mu}_s n_s}}{dr} = \frac{d[W_{\tilde{\mu}_s n_s} + PV_{ni}]}{dr} - 8\pi(\tilde{\gamma} - \gamma)(r - l) \quad (14)$$

where l is a positive quantity that would be a combination of $\tilde{\delta}$ and δ. This length depends on the limiting density profile of the cavity/water interface. Equations 12 and 14 will be used to check the validity of the decomposition above based on the assumption made on $f_c(r)$. Although we will discuss the quantities in eqs 12 and 14 only qualitatively in terms of the simulation results of ΔV_{ni},[27] this will permit us to have an insight on $\tilde{\mu}_s$. In fact, if $\tilde{\mu}_s$ is constant, $W_{\tilde{\mu}n_s}$ and its derivative with respect to r can easily be derived from the known behavior of ΔV_{ni}.

On the basis of the assumptions made above, $t(r)$ and $\zeta(r)$ play a role in eqs 12 and 14. In particular, for the latter, we have

$$\frac{d\tilde{W}_{\tilde{\mu}n_s}}{dr} = 8\pi\tilde{\gamma}t(r)(r - \tilde{\delta}\, e^{-\delta_1/r}) - 8\pi\tilde{\gamma}(r - \tilde{\delta}) \quad (15)$$

from which the ratio ϕ between the $d\tilde{W}_{\mu n_s}/dr$ and $d\tilde{W}_s/dr$ is obtained

$$\phi = t(r)\frac{r - \delta\, e^{-\delta_1/r}}{r - \delta} - 1 \quad (16)$$

The exponential thus controls the crossover to the asymptotic behavior of the derivative that is reached at $r \gg \delta_1$, when ϕ tends to 0.

3.2. Connecting to the Microscopic Limit. In this work, we propose for $t(r)$ the following expression

$$t(r) = \exp(a\, e^{-r/\delta_0} + b\, e^{-(r/\delta_0)^{1/m}}) \quad (17)$$

where a, b, δ_0, and m are parameters. This function is 1 at infinity and tends to 0 at $r = 0$ provided $a + b$ has an appropriate negative value. Nevertheless, it achieves the correct value at $r = 0$ in the wrong way. To correct this limit for the second derivative at $r = 0$, we join eq 9 with the known exact expression for subatomic cavities coming from SPT by means of the Heaviside step function. With this assumption, eq 9 becomes

$$\frac{dW}{dr} = \rho_0 k_B T 4\pi r^2 G_{SPT}(r)[1 - H(r - r_0)] + 8\pi\gamma t(r)(r - \delta\, e^{-\delta/r})H(r - r_0) + 4\pi r^2 P \quad (18)$$

where

$$H(r - r_0) = \begin{cases} 0, & r < r_0 \\ 1, & r \geq r_0 \end{cases} \quad (19)$$

and $G_{SPT}(r)$ is computed by eq 5. For $r < r_0$, the expression above gives the exact behavior predicted by SPT when no triplets of oxygens can be found in the cavity. Equation 9 can also give a good description at shorter radii when no pairs can be found in the cavity, and G_{SPT} has the simple expression

$$G_{SPT}(r) = \frac{1}{1 - \rho_0\left(\frac{4}{3}\pi r^3\right)} \quad (20)$$

The requirement of a continuous and smooth transition from microscopic to macroscopic behaviors[20,41] put limits on the choice of r_0. The continuity and smooth conditions could also be exploited to fix two parameters of the model, even if this could be less convenient than a determination by fitting.[29] The limiting expression can also be reached smoothly from eq 9 by means of the hyperbolic tangent. So, as an alternative to eq 18, we can use

$$\frac{dW}{dr} = \frac{\rho_0 k_B T 4\pi r^2[1 - \xi(r;r_0,d_0)]}{1 - \rho_0\left(\frac{4}{3}\pi r^3\right)[1 - \xi(r;r_1,d_1)]} + 8\pi\tilde{\gamma}t(r)(r - \tilde{\delta}\, e^{-\delta_1/r})\xi(r;r_0,d_0) + 4\pi r^2 P \quad (21)$$

where

$$\xi(r;r_0,d_0) = \frac{1}{2} + \frac{1}{2}\tanh\left(\frac{r - r_0}{d}\right) \quad (22)$$

in which the step function $H(r,r_0)$ is regained by putting $d_0 = 0$. Note that $\xi(r;r_1,d_1)$ in eq 21 avoids divergences in the first term. The parameters r_0, d_0, r_1, and d_1 must be appropriately fixed to guarantee that the transition between the two limiting behaviors occur without any discontinuity and smoothly. By insertion of eqs 18 and 21 into eq 2, the corresponding expression for $G(r)$ is obtained. According to SPT,[20] the cavitation free energy of a spherical cavity can be obtained by integrating its derivative with respect to the radius. From eqs 18 and 4, we get

$$W(r) = W_{micro}(r)[1 - H(r - r_0)] + \left[c + 4\pi\tilde{\gamma}r^2 t(r) + 4\pi\gamma\int_{r_0}^{r} ds\, s^2 t(s)\left(a\, e^{-s} + b\frac{e^{-s^{1/m}}}{m s^{1-1/m}}\right) - 8\pi\tilde{\gamma}\tilde{\delta}\int_{r_0}^{r} ds\, e^{-\delta_1/s}\, t(s)\right]H(r - r_0) + \frac{4}{3}\pi r^3 P \quad (23)$$

where the microscopic contribution, according to eq 4, can be computed by

$$W_{micro}(r) = -k_B T \ln\left[1 - \rho_0\left(\frac{4}{3}\pi r^3\right) + (\pi\rho_0)^2\int_0^{2r} ds\, g_{OO}(s)(s^5/6 - 2r^2 s^3 + 8r^3 s^2/3)\right] \quad (24)$$

and c is a constant given by

$$c = W_{micro}(r_0) - 4\pi\tilde{\gamma}r_0^2 t(r_0) \quad (25)$$

With r_0 in the limit of very small cavities, the microscopic contribution is the well-known limit predicted by SPT, namely,

$$W_{micro}(r) = -k_B T \ln\left[1 - \rho_0\left(\frac{4}{3}\pi r^3\right)\right] \quad (26)$$

By integrating eq 21, we obtain the ensuing expression

$$W(r) = \rho_0 kT 4\pi \int_0^r \mathrm{d}s \frac{s^2[1-\xi(s;r_0,d_0)]}{1-\rho_0\left(\frac{4}{3}\pi s^3\right)[1-\xi(s;r_1,d_1)]} + 4\pi\tilde{\gamma} r^2 t(r)\xi(r) + 4\pi\tilde{\gamma}\int_0^r \mathrm{d}s\, s^2 t(s)\left[\xi(s)\left(a\,\mathrm{e}^{-s} + b\frac{\mathrm{e}^{-s^{1/m}}}{ms^{1-1/m}}\right) - \frac{1}{2d}\frac{1}{\cosh^2\left(\frac{s-r_0}{d}\right)}\right] - 8\pi\tilde{\gamma}\tilde{\delta}\int_0^r \mathrm{d}s\, \mathrm{e}^{-\delta_1/s}\, t(s)\xi(s) + \frac{4}{3}\pi r^3 P \quad (27)$$

4. Results and Discussion

4.1. *G*(*r*) and the Derivative of the Cavitation Free Energy. Radial distribution functions for several hard-sphere cavities in TIP4P water were obtained from Monte Carlo (MC) simulations in the isothermal, isobaric ensemble at 298 K and 1 atm. A wide range of radii were explored from 0.95 Å up to 10 Å. Some details of these MC simulations are shown in Table 1. Water−water interactions were truncated at half the simulation box length except for the largest box of 1435 molecules, for which the same cutoff of the box of 512 molecules was used. No significant size box effects were observed in the two cases with $r = 3.3$ Å and $r = 3.45$ Å, for which the calculated rdf's with 216 and 512 molecules are in agreement within the statistical uncertainties. A slightly modified version of BOSS program[15,57] was used. As in other works,[27,58] rdf's from BOSS were renormalized by the scaling ρ/ρ_0, where ρ was the density used by the program and ρ_0 the density of pure water computed with the same number of molecules used in the simulated solution. MC simulations were very long to obtain good accuracy in $G(r)$ values. Statistical errors were evaluated as standard errors in the block averages after the variance had been analyzed with the block length to evaluate sampling correlations. In the worst case, the error on the contact value of the rdf is of about 2%.

The values of $G(r)$ versus the cavity radius are plotted in Figure 1. According to eqs 2, 5, and 18, $G(r)$ must be 1 at $r = 0$ and tend to 0 at infinity,[9] $P/(\rho_0 k_B T)$ being a negligible quantity. The latter comes from the derivative of the $P\Delta V$ term in the Gibbs free energy and is very small in terms of the conditions of the systems studied here. Between the two limit values, $G(r)$ has a maximum around 2.8 Å, which is in agreement with other simulation results.[9,43]

Derivatives of W were obtained from $G(r)$ via eq 2 and are plotted against the cavity radius in Figure 2. Uncertainties on contact values $G(r)$ were propagated to obtain uncertainties on the derivative of cavitation free energies. For the moment, we have limited the choice of m to some integer value. The weighted least squares were used to fit the data through eq 9 with $m = 2$, 3, and 4 and $b = -a/10$. We have found it convenient to fix $\delta_1 = \tilde{\delta}$ in $\zeta(r)$ and $\delta_0 = 1$ Å in $t(r)$. The optimized parameters, $\tilde{\gamma}$, a, and $\tilde{\delta}$, are shown in Table 2, together with some statistical information on the quality of the above fitting. The table highlights that eq 9 performs very well without significant differences among the three values of m considered. Checking the residuals confirmed this conclusion, as we found them randomly distributed around 0. Moreover, they fall mainly within σ_i, the statistical uncertainties of simulation results, and only a few points fall outside, but in any case they are within $2\sigma_i$. Nevertheless, Figure 2 also shows that larger residuals were obtained for cavity radii of 7.05 and 10 Å for which systematic errors due to box size cannot be completely ruled out. In any case, the low values of such errors did not change our conclusion. The quality of the fitting is not substantially affected by these two points.

TABLE 1: Contact Values from MC Simulations[a] for Hard-Sphere Solute−TIP4P Oxygen rdf's

r_{hs} (Å)	N_w	$g(r_{hs})$	r_{hs} (Å)	N_w	$g(r_{hs})$
0.95	216	1.192 ± 0.012	4.05	512	1.975 ± 0.019
1.25	216	1.424 ± 0.015	4.45	512	1.855 ± 0.016
1.45	216	1.660 ± 0.012	4.70	512	1.792 ± 0.010
1.75	216	1.888 ± 0.015	5.05	512	1.723 ± 0.008
1.90	216	1.967 ± 0.011	5.45	512	1.619 ± 0.007
2.00	216	2.026 ± 0.010	6.05	512	1.467 ± 0.007
2.25	216	2.154 ± 0.013	6.50	512	1.372 ± 0.018
2.55	216	2.191 ± 0.010	7.05	512	1.263 ± 0.017
2.85	216	2.192 ± 0.010	7.50	1435	1.222 ± 0.015
3.00	216	2.146 ± 0.011	8.00	1435	1.163 ± 0.020
3.30	216	2.145 ± 0.011	8.50	1435	1.079 ± 0.018
3.30	512	2.157 ± 0.019	9.00	1435	1.041 ± 0.015
3.45	216	2.108 ± 0.011	9.50	1435	0.983 ± 0.022
3.45	512	2.126 ± 0.012	10.0	1435	0.904 ± 0.013

[a] The numbers of configurations used in the averages were between 5×10^9 and 5×10^{10}.

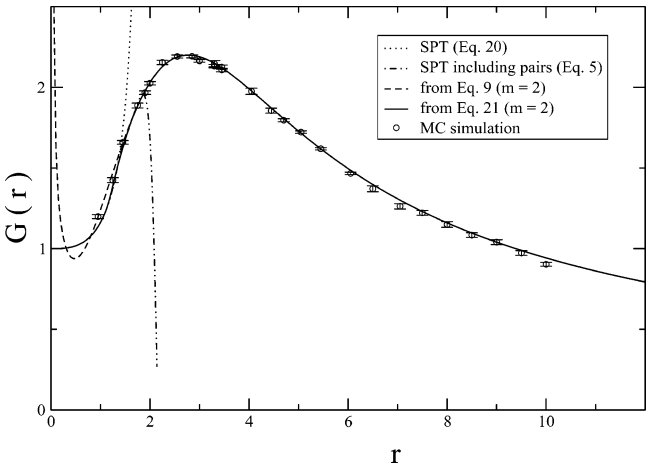

Figure 1. Contact values of the cavity−TIP4P oxygen rdf's versus cavity radii (Å) from MC simulation data and comparison with the results obtained via eq 2 from derivatives computed by using eqs 9 and 21 with the choice $b = -a/10$ and $m = 2$. Curves from exact expressions holding in the region of very small cavities derived from SPT are also shown.

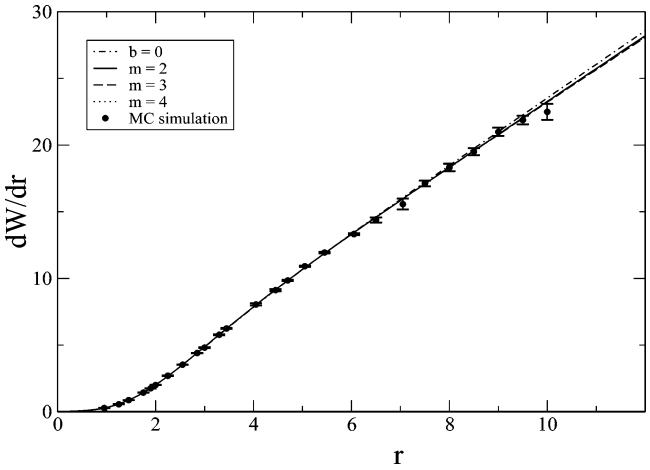

Figure 2. Derivative of cavitation free energies (kcal/mol) with respect to the cavity radius (Å) obtained from MC simulation data of $G(r)$ via eq 2 and comparison with curves of the fittings with eq 9 for different fixed values of b and m (see also Table 2). Where not specified $b = -a/10$.

TABLE 2: Nonlinear Weighted Least Squares Fit with Eq 9 of d*W*/d*r* Derived from MC Simulation Data of Contact Values of Hard-Sphere Solute−TIP4P Oxygen rdf's, Optimized Parameters ($\tilde{\gamma}$, *a*, and $\tilde{\delta}$), and the Reduced χ^2, χ_ν^2, for Different Fixed Values of *m* and *b* (See Text and Notes)

range [Å]	*m*	γ [dyn/cm]	*a*	$\tilde{\delta}$ [Å]	χ_ν^2
[0.95,10]	2[a]	69.4 ± 0.4	−4.98 ± 0.02	1.03 ± 0.03	1.05124
[0.95,10]	3[a]	66.7 ± 0.4	−4.85 ± 0.02	0.99 ± 0.03	1.03345
[0.95,10]	4[a]	64.9 ± 0.4	−4.78 ± 0.02	0.95 ± 0.03	1.07246
[0.95,10]	[b]	70.1 ± 0.5	−4.58 ± 0.03	0.78 ± 0.04	1.59616

[a] $b = -a/10$. [b] $b = 0$.

Judging only on the basis of the quality of the fitting, there is no particular value of *m* to prefer of the three chosen, though the model performs slightly better with $m = 3$. Some discrimination would be in principle possible if the range of the data were extended to larger radii, where unfortunately simulations become too expensive. Moreover, this might not actually be very helpful given the accuracy currently accessible in computer simulations. In fact, discrepancies between $G(r)$ predicted by different *m*'s are very small even for very large cavities. On the other hand, $m = 2$ gives a value of $\tilde{\gamma}$ closer to the surface tension computed from simulations of liquid−vapor interface for the TIP4P model (70.2 ± 1.7 dyn/cm [59]) at 293 K. The agreement is also very good considering that γ decreases with *T*. In principle, a hard wall interface and a liquid−vapor interface can have different values of surface tension. In particular, a higher value is expected for a hard wall because of a possible inhibition of density fluctuations in the interfacial region.[16,43] This was found by Ashbaugh and Paulaitis[43] who fitted MC simulation data of $G(r)$ for SPC water with a simple model consistent with eq 3.

However, Huang et al.[16] have supported the idea that there are no substantial differences between the two interfaces for water at room temperature and 1 atm pressure and predicted the same value of surface tension, in agreement with Stillinger's[41] suggestion. Our extrapolated value of γ gives further support to this second view. Given the slight dependence of the quality of the fitting on the value of *m*, we also considered the case with $b = 0$ (see Table 2). Although residuals are in general higher than in the other cases, χ_ν^2 is not increased enough to reject this simpler model on the basis of the quality of the fitting. This model gives a value of surface tension in agreement with that obtained with $m = 2$ but with a smaller value of $\tilde{\delta}$. As mentioned in the previous section, eq 9 tends to 0 in a wrong way. On the scale of Figure 2, this cannot be seen. However, although a comparison with values obtained from eq 20 shows only small errors for $r < 1$ Å, there was nevertheless some trend in this region. This becomes clearer by comparing $G(r)$ obtained from eq 9 with the correct behavior at $r = 0$, as shown in Figure 1. The new model crosses the curve obtained from the correct expression for a microscopic cavity (eq 5) at 0.83 and at 1.73 Å. This latter gives the appropriate value for r_0 in eq 18. We note that in this region, also, simulation results disagree with SPT in the same way as the model from eq 9. However, for radii between these values, the maximum error is only 6%. So, in eq 18, we can neglect the contribution of pairs to $G_{SPT}(r)$ (eq 20). In this case, the best value for r_0 is 1.3 Å because discrepancies are still smaller in the region between this value and 1.73 Å. The same value of r_0 is appropriate in eq 21 in combination with $d_0 = d_1 = 0.12$ Å and $r_1 = 1.45$ Å. This model permits a continuous and smooth transition between SPT and eq 9 in the limit of subatomic cavities. Figure 1 shows that it behaves properly in the region where we cannot neglect pairs contribution.

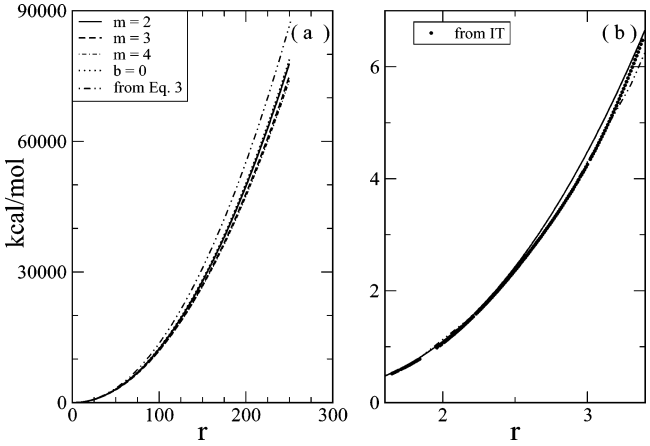

Figure 3. (a) $W(r) - P(4\pi r^3/3)$ obtained from the new model (eq 23) for different fixed values of *m* and *b* and parameters γ, *a*, and $\tilde{\delta}$ optimized by fitting (see Table 2). A comparison is also done with the simple model defined by eq 3 with parameters optimized by fitting simulation data for radii larger than 1.75 Å (see Table 5). This model has been combined with the exact expression of SPT (eq 4). Panel b presents the same parameters as panel a, but in the scale of small cavities. In this region, there are not visible differences between different choices of *m* and *b*. A comparison with results from information theory (IT) is included (see Table 3). Radii are in Å.

4.2. The Cavitation Free Energy. Values of $W(r) - P(4/3)\pi r^3$ are plotted in Figure 3a. This set of data was obtained by numerical integration of eq 18 with an integration step sufficiently small (5×10^{-4} Å) to guarantee a good accuracy. A preliminary study for $r < 25$ Å showed that a step integration of 5×10^{-2} Å gives an accuracy in $W(r)$ of $\sim 10^{-5}$ kcal/mol. Instead we did not make a rigorous propagation of parameter errors on $W(r)$, but an approximate estimate showed that these were very small. However, different choices for *m* and *b* can produce discrepancies in $\tilde{\gamma}$ that are over the uncertainty of the parameter, but as for the derivative, they give very close results in the range of the simulation data. Disagreement between them becomes evident for a cavity radius larger than 40 Å. Although discrepancies increase with the radius, they appear to be negligible in comparison with the value of *W* itself. For example, discrepancies are about 4% at 250 Å between $m = 2$ and $m = 3$. Note that these are essentially due to the different fitted values of $\tilde{\gamma}$. As an additional test on the goodness of the model, we compared the results with the cavitation free energies computed by using information theory (IT).[48] The latter were obtained by using the flat default model[48] and including contributions up to the second moment of O−O density of TIP4P water. It is well-known from the literature that this approximation gives free energies in agreement with simulations for cavities with radius up to ~3.2 Å. A comparison was thus made in this range. Examining the root of the mean square errors shows a substantially good agreement for all choices of *b* and *m* (see Table 3). Nevertheless, the small deviations do no appear to be randomly distributed as shown in Figure 3b.

To interpret the new expression for $W(r)$, we prefer to rewrite eq 23 in the following way

$$W(r) = W_{\text{micro}}(r)[1 - H(r - r_0)] + [c' + 4\pi\gamma r^2 t(r) + W_{b,m}(r) + W_{\tilde{\delta}}(r)]H(r - r_0) + \frac{4}{3}\pi r^3 P \quad (28)$$

where $W_{b,m}(r)$ and $W_{\tilde{\delta}}(r)$ depend on parameters *b*, *m*, and $\tilde{\delta}$ and come from the integrals

$$W_{b,m}(r) = 4\pi\gamma\int_0^r \mathrm{d}s\, s^2 t(s)\left(a\, \mathrm{e}^{-s} + b\frac{\mathrm{e}^{-s^{1/m}}}{ms^{m-1/m}}\right) \quad (29)$$

and

$$W_{\tilde{\delta}}(r) = -8\pi\tilde{\gamma}\tilde{\delta}\int_0^r \mathrm{d}s\, \mathrm{e}^{-\tilde{\delta}/s}\, t(s) \quad (30)$$

The integration constant c', which depends on r_0, is given by

$$c' = W_{\mathrm{micro}}(r_0) - 4\pi\gamma r_0^2 t(r_0) - W_{b,m}(r_0) - W_{\tilde{\delta}}(r_0) \quad (31)$$

We found that it is a negligible quantity for $r_0 = 1.3$ Å for all values of b and m considered in this work. According to the assumptions made in section 3, precisely in eq 6 and the ensuing equations, $W_{b,m}$ must be associated with the term proportional to the excess number of molecules on the dividing surface (n_s). The constant c' might include a constant associated with the Gaussian curvature, but the discussion of this term goes beyond the scope of this paper. Thus we will not ascribe components of c' to the surface contribution, as defined below, and consequently to the complementary term because it would not be sufficiently supported. In addition, we neglect c', since its value is less than or equal to 0.01 kcal/mol. In line with eqs 13 and 14 for $r > r_0$, we discuss the quantities

$$\tilde{W}_s = \tilde{\gamma}\left(1 - 2\frac{\tilde{\delta}}{r}\right)(4\pi r^2) \quad (32)$$

and

$$\tilde{W}_{\tilde{\mu}_s n_s} = 4\pi\tilde{\gamma}r^2[t(r) - 1] + W_{b,m}(r) + [W_{\tilde{\delta}}(r) + 8\pi\tilde{\gamma}\tilde{\delta}r] \quad (33)$$

Surface tension values depending on the cavity radius obtained from eq 32 simply dividing by the spherical surfaces are plotted in Figure 4. Within the error of $\tilde{\gamma}$, the convergence to the asymptotic limit is reached at $r \approx 300$ Å. Although rates of convergence are quite similar for the different chosen values of m and b, the convergence is faster for $b = 0$.

In contrast, a detailed analysis shows that different values of m and b produce very different terms of $\tilde{W}_{\tilde{\mu}_s n_s}$ (Figure 5a,b). For example, $W_{b,m}$ converges to different asymptotic values depending on the particular value of m and b. Note also that a much more rapid convergence is observed for higher values of $\tilde{\gamma}$ (see Table 2). Therefore, the knowledge of $\tilde{W}_{\tilde{\mu}_s n_s}$ in the limit of large cavities would lead to a correct choice of m and b. Nevertheless, the value of b is important also for cavities of small radius as shown in the plot of $W_{b,m}$. In the case of $\tilde{\gamma} = \gamma$ and $\tilde{\mu}_s$ constant, we would be able to draw immediately a conclusion. In fact, for the accessible surface, n_s differs from ΔV_{ni} only for a scaling factor and for the sign. Therefore, in the reasonable case of a negative value of $\tilde{\mu}_s$, $W_{\tilde{\mu}_s n_s}$ and $P\Delta V_{ni}$ behave qualitatively in the same way. In agreement with our previous calculations of ΔV_{ni},[27] $\tilde{W}_{\tilde{\mu}_s n_s}$ should be negative for a radius smaller than ~8.5 Å with a flat minimum at ~5.5 Å. The addition of a constant to $\tilde{W}_{\tilde{\mu}_s n_s}$ can have effect on the radius at which the change in sign is observed. However, the radius at which the minimum is observed could be justified on the basis of the hypotheses made above. A flat minimum was observed at ~3 Å for $b \neq 0$ and at 5.3 Å for $b = 0$. For a complete discussion, we consider also the derivative that we expect to be negative for cavities with radius smaller than ~5.5 Å. For $r \geq r_0$, we found that the derivative was negative up to ~ 3 Å for $b \neq 0$ and up to ~5.3 Å for $b = 0$. Thus we arrive at the conclusion that the model for $b = 0$ is consistent with the simple picture delineated by the two hypotheses above. On the other hand, the behavior observed for $b \neq 0$ could be justified with a dependence on r of $\tilde{\mu}_s$. In fact, the term proportional to $\tilde{\gamma} - \gamma$ in eq 14 can only extend the region of negatives values beyond 5.5 Å.

Finally, Figure 6a,b shows, respectively, ϕ in eq 16 and the quantity $\tilde{W}_{\tilde{\mu}_s n_s}/\tilde{W}_s$ against the cavity radius. The curves have been plotted for radii larger than $2\tilde{\delta}$. In fact, for smaller radii, we are not sure whether we can attribute physical meaning to the interpretation above, because we expect positive values of $\tilde{W}_s$. This is a consequence of the assumption made on $f_c(r)$ that includes only curvature corrections on the order of $1/r$. When $b \neq 0$, ϕ shows a maximum, and the ratio of the free energy

TABLE 3: Root Mean Square Error (rmse) by Comparing Models Parametrized on dW/dr Data to Cavitation Free Energies from Information Theory Results for Cavities with Radius in the Range [1.76, 3.22] Å

model	rmse
eq 23 ($m = 2$)	0.134
eq 23 ($m = 3$)	0.134
eq 23 ($m = 4$)	0.134
eq 23 ($b = 0$)	0.135
eq 27 ($m = 2$)	0.137
eq 34[a]	0.120
eq 34[b]	0.054
eq 34[c]	0.067

[a] Parameters obtained by fitting eq 34 (see Table 4) to results of dW/dr derived from MC simulations. [b] γ fixed at 80 dyn/cm and the other two parameters obtained by imposing continuity between eq 5 and eq 34 at 1.8 Å ($\tilde{\delta} = 1.49$ Å and $\alpha = 1.45$ Å^3). [c] γ fixed at 70 dyn/cm and the other two parameters obtained by imposing continuity between eq 5 and eq 34 at 1.8 Å ($\tilde{\delta} = 1.32$ Å and $\alpha = 0.82$ Å^3).

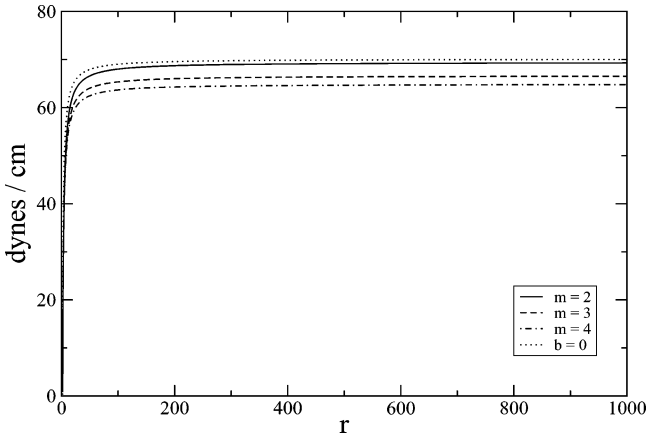

Figure 4. $\tilde{W}_s/(4\pi r^2)$ versus the cavity radius (Å).

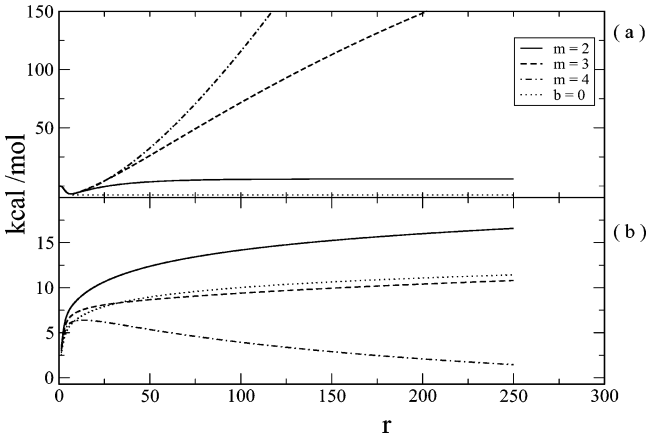

Figure 5. (a) $W_{b,m}$ (see eq 29) versus the cavity radius (Å) and (b) $W_{\tilde{\delta}} + 8\pi\tilde{\gamma}\tilde{\delta}r$ versus the cavity radius (see eqs 30 and 33).

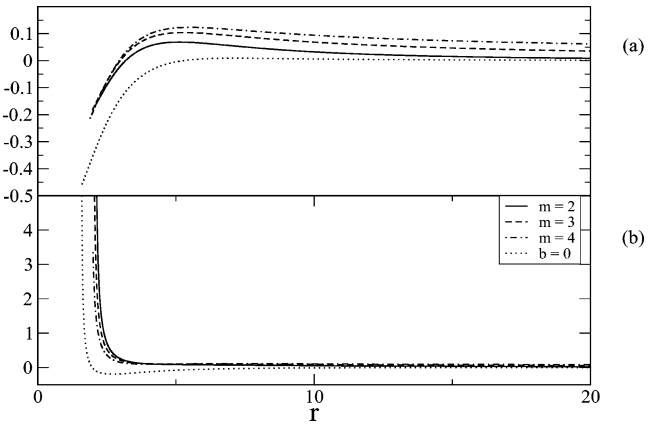

Figure 6. (a) Dependence on the cavity radius (Å) for the ratio ϕ between derivative contributions (see eq 16) coming from the term proportional to n_s (see eq 33) and that from $\tilde{W}_s$ (see eq 32) and (b) the same for the ratio between the corresponding free energy contributions.

TABLE 4: Linear Weighted Least Squares Fit of d*W*/d*r* Derived from MC Simulation Data of Contact Values of Hard-Sphere Solute−TIP4P Oxygen rdf's, Optimized Parameters (γ and $\tilde{\delta}$), and the Reduced χ^2, χ_ν^2

range [Å]	γ [dyn/cm]	$\tilde{\delta}$ [Å]	χ_ν^2
[0.95,10]	60 ± 2.7	0.89 ± 0.06	785.811
[6.05,10]	69.6 ± 1.1	0.8 ± 0.1	0.521154

components is always positive. Instead, both quantities behave in a qualitatively different way when $b = 0$. We note also that the convergence rate of ϕ considerably depends on the chosen values of b and m. Moreover, in all cases, values of $\tilde{W}_{\mu n_s}$ are quite relevant as they vary from $\sim k_B T$ to quantities that may even be much larger than $k_B T$ depending on the choices of b and m.

4.3. Comparison with Simple Models. Let us consider first the cavitation free energy as given in eq 1 to obtain contact values of rdf's via eq 2. The two parameters of the model were obtained by fitting the derivative of $W(r)$ with a straight line. The resulting values of $\tilde{\gamma}$ and $\tilde{\delta}$ are collected in Table 4, together with some statistical details to evaluate the quality of the fitting procedure. Since the model is appropriate for a macroscopic spherical cavity, we have considered the dependence of the parameters values on the range of the cavity radius. When this includes microscopic cavities up to a minimum contact radius of 0.95 Å, as expected, a bad performance of the model is observed. The resulting contact values of rdf's compared to MC simulation results show the inadequacy of the model for microscopic cavities with a radius less than ∼4 Å. If the data collected in this range are excluded, only $\tilde{\gamma}$ changes significantly. In particular, it increases to a value of ∼70 dyn/cm, which is in agreement with the value obtained by Zhang et al.[59] from a simulation of the liquid/vapor interface with the TIP4P model. This is also in agreement with the values obtained with the new model proposed in this paper when $m = 2$ ($b = -a/10$) and when $b = 0$ (see Table 2). Huang et al.[16] found similar values from simulation results in the same range for SPC/E[60] water ($\tilde{\gamma} = 71.8 \pm 0.8$ dyn/cm and $\tilde{\delta} = 0.90 \pm 0.03$ Å).

Next, we fit the derivative of the free energy with the expression that is consistent with eq 3, namely,

$$\frac{dW}{dr} = 4\pi\tilde{\gamma}\left(2r - 2\tilde{\delta} + \frac{\alpha}{r^2}\right) \tag{34}$$

The quality of the fitting is much worse than that performed by the new model (eq 9). The residuals show some trend and are

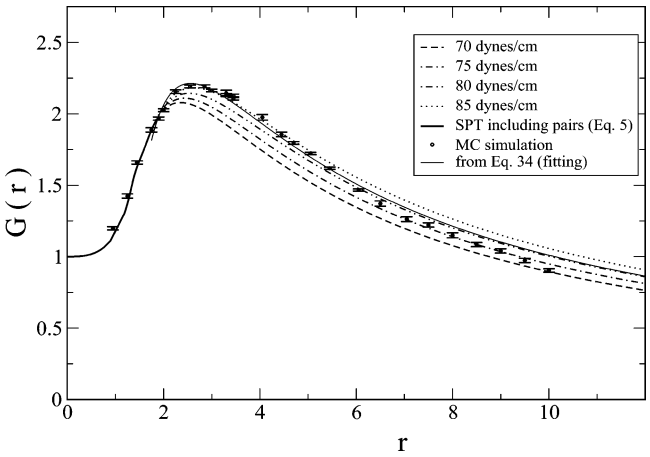

Figure 7. $G(r)$ curves versus cavity radius (Å) obtained via eq 2 from derivatives of $W(r)$ modeled with eq 34 for different fixed values of γ. Parameters $\tilde{\delta}$ and α were obtained by imposing continuity at 1.8 Å with eq 5.

TABLE 5: Nonlinear Weighted Least Squares Fit with Eq 34 of the d*W*/d*r* Data Derived from MC Simulation Data of Contact Values of Hard-Sphere Solute−TIP4P Oxygen rdf's, Optimized Parameters ($\tilde{\gamma}$, $\tilde{\delta}$, and α), and the Reduced χ^2, χ_ν^2 Illustrating the Parameters' Dependence on the Range

range [Å]	$\tilde{\gamma}$ [dyn/cm]	$\tilde{\delta}$ [Å]	α [Å^3]	χ_ν^2
[0.95,10]	80.2 ± 0.8	1.41 ± 0.01	0.99 ± 0.03	21.5476
[1.75,10]	79.7 ± 1.2	1.36 ± 0.05	0.5 ± 0.3	11.4946
[1.90,10]	78.5 ± 1.1	1.29 ± 0.05	-0.0003 ± 0.3	9.12128

mainly larger than uncertainties of the simulation data. These behaviors change only a little bit (see Table 5) if some points in the region of the smaller cavities are excluded. In this case, the addition of the term proportional to $1/r^2$ significantly improves the description in the region of microscopic cavities with a radius <4 Å when data are compared with the linear fit of the derivative, as can be seen in Figure 7. Note that $\tilde{\gamma}$ is now significantly higher than the value found for the liquid−vapor interface. However, this is expected because Pratt and Pohorille[42] and Ashbaugh and Paulaitis[43] found the same using the same model. Significant differences are shown also for $\tilde{\delta}$ by comparison with eq 9 (Table 2) and with the straight line fitting (Table 4). In addition, the value of α depends significantly on the range, becoming practically zero when radii smaller than 1.95 Å were not considered.

An alternative procedure to the fitting consists of determining $\tilde{\delta}$ and α by interpolation between microscopic and macroscopic limits. Continuity of $G(r)$ and its derivative has been imposed between the expression derived from eq 34 via eq 2 and the expression derived from the SPT[20] (eq 5), which is exact for a cavity radius less than ∼1.9 Å. This procedure was suggested by Stillinger[41] and has already been used in the literature.[42,43] We show the curves of the contact values of rdf obtained for different values of $\tilde{\gamma}$, imposing the two continuity conditions at 1.8 Å. The plot shows that it is not possible to obtain a good agreement with the simulation results in all the range with a unique value of $\tilde{\gamma}$. In fact, a value of ∼85 dyn/cm is appropriate for small cavities with a radius less than ∼5 Å, while a value of 70−75 dyn/cm appears to be more appropriate for larger cavities. The presence of some degree of indetermination in $\tilde{\gamma}$ when the continuity is imposed seems to indicate that the model is inadequate in some way.

After integration of eq 34, cavitation free energies can be obtained by adding the proper constant w_0, whose value depends on the radius chosen for the joint with the correct expression in the region of the smaller cavities. Finally, the comparison of

$W(r)$ with free energies coming from information theory is very good and in fact is slightly better than that found with the new model previously discussed (see Figure 3b and Table 3). Nevertheless, although deviations are very small, they do show some trends thus indicating systematic errors.

5. Conclusions

In the framework of the thermodynamics of surfaces, we have derived a new expression for the cavitation free energy by integrating a new model for its derivative with respect to the cavity radius. Because the accessible surface is in principle noncoincident with the equimolar surface, the term proportional to the excess number of molecules at the dividing surface has been taken into account. This has been assumed to behave as a quadratic function of r in the large size limit. Consequently, the asymptotic behavior of the derivative is the same as that of the classic expression for a macroscopic cavity. This is parametrized in terms of $\tilde{\gamma}$ and $\tilde{\delta}$, whose values are in principle affected by the contribution due to the asymptotic behavior of the term depending on n_s. By a proper scaling of $\tilde{\delta}$, the transition from small to large length scales has been described by a factor $t(r)$, which is zero at $r = 0$ and 1 at infinity. For the typical expression used to describe the curvature correction of the surface tension, $t(r)$ and the scaling factor $\zeta(r)$ enter into the description of the term depending on n_s. Thus, additional information on the behavior of this term can be useful in searching and parametrizing $t(r)$.

The functional form proposed for $t(r)$ depends on four parameters, m, a, b, and δ_0, but only one of them (a) was optimized in the fitting procedure applied to the derivative data from MC simulations. Thus the complete function defines a model with three parameters, a, $\tilde{\gamma}$, and $\tilde{\delta}$. In the most simple version of the model, $b = 0$. In the other cases, $b = -a/10$, for which three different choices of m (2, 3, and 4) have been considered. These different choices determine different rates of convergence to the asymptotic limit of the derivative. The fitting has also shown that they correspond to different values of $\tilde{\gamma}$, while $\tilde{\delta}$ on the other hand is always close to 1 Å. There are no significant differences in the quality of the fitting, which is generally very good. However, with $m = 2$ we have obtained a value of $\tilde{\gamma}$ that is in very good agreement with the surface tension obtained from simulation calculations on the liquid−gas interface. This also happens when $b = 0$, but the quality of the fit is not as good.

The new model has limitations for radii smaller than 1 Å, where a comparison with the exact expression coming from SPT has been made. Discrepancies in this region are small for the derivative, but are relevant for $G(r)$. Consequently, the new model can be combined with the exact expression from SPT by means of a step function. On the other hand, other functions permit a continuous transition between the two expressions. The switch between the two expressions appears most suitable at 1.3 Å. However, a contact distance of 1 Å corresponds approximately to a point solute in contact with TIP4P oxygen, which is rarely considered in the usual applications of chemical interest.

Finally, we interpret the cavitation free energy in terms of a surface term and the complementary term depending on the excess number of molecules at the dividing surface. We have limited the discussion to the assumption of a curvature factor that includes the most important curvature correction. So, the given decomposition appears to have physical meaning for contact radii larger than $2\tilde{\delta}$. We have found that $\tilde{W}_{\tilde{\mu}_s n_s}$ is a relevant quantity, which varies from $\sim k_B T$ to values that may even be very much larger than $k_B T$, depending on the choices of b and m. Additional information on this term appears important for a discrimination between different choices of b and m. Here, a partial examination at a qualitative level has shown that the choice with $b = 0$ seems to be consistent with the most simple picture corresponding to $\tilde{\mu}_s$ constant and $\tilde{\gamma} = \gamma$. Nevertheless, we need a deeper analysis to arrive at a definite decision.

In conclusion, the new model performs much better than the functional form proposed by Stillinger[41] and subsequently used by Pratt and Pohorille[42] and more recently by Ashbaugh and Paulaitis.[43] This functional form appears slightly better than the new model only when a comparison of cavitation free energies to results from information theory is made in the limited range between 2 and 3.2 Å. Moreover, with this model the optimized value of surface tension is 80.2 dyn/cm, which is significantly higher than the computed value for the liquid/vapor interface. Following Stillinger, Huang et al.[16] supported the idea that at ambient conditions for water practically no difference would be expected in the value of the surface tension between the liquid−vapor interface and a liquid−vacuo interface described by a rigid wall. In this view, our new model would be suitable for describing the transition from microscopic to macroscopic cavities.

Acknowledgment. The author acknowledges Dr. Claudio Amovilli for useful discussions. Finally, a referee made numerous constructive comments, which have improved the presentation of this work, and the author is grateful to him for his interest.

References and Notes

(1) Blokzijl, W.; Engberts, J. B. F. N. *Angew. Chem., Int. Ed. Engl.* **1993**, *32*, 1545.
(2) Berne, B. *Proc. Natl. Acad. Sci. U.S.A.* **1996**, *119*, 8800.
(3) Smith, P. *J. Phys. Chem. B* **1999**, *103*, 525−534.
(4) Hummer, G.; Garde, S.; García, A.; Pratt, L. *Chem. Phys.* **2000**, *258*, 349−370.
(5) Southall, N. T.; Dill, K. A.; Haymet, D. J. *J. Phys. Chem. B* **2002**, *106*, 521.
(6) Postma, J.; Berendson, H.; Haak, J. *Faraday Symp. Chem. Soc.* **1982**, *17*, 55.
(7) Straatsma, T.; Berendson, H.; Postma, J. *J. Chem. Phys.* **1986**, *85*, 6720.
(8) Pohorille, A.; Pratt, L. *J. Am. Chem. Soc.* **1990**, *112*, 5066.
(9) Pratt, L.; Pohorille, A. *Proc. Natl. Acad. Sci. U.S.A.* **1992**, *89*, 2995.
(10) Lee, B. *Biophys. Chem.* **1994**, *51*, 271.
(11) Madan, B.; Lee, B. *Biophys. Chem.* **1994**, *51*, 279.
(12) Beutler, T.; Béguelin, D.; van Gunsteren, W. *J. Chem. Phys.* **1995**, *102*, 3787.
(13) Wallqvist, A.; Berne, B. *J. Phys. Chem.* **1995**, *99*, 2885.
(14) Prèvost, M.; Oliveira, I.; Kocher, J.; Wodak, S. *J. Phys. Chem.* **1996**, *100*, 2738.
(15) Floris, F.; Selmi, M.; Tani, A.; Tomasi, J. *J. Chem. Phys.* **1997**, *107*, 6353.
(16) Huang, D.; Geissler, P.; Chandler, D. *J. Phys. Chem. B* **2001**, *105*, 6704−6709.
(17) Huang, D.; Chandler, D. *J. Phys. Chem. B* **2002**, *106*, 2047−2053.
(18) Pratt, L.; Chandler, D. *J. Chem. Phys.* **1977**, *67*, 3683.
(19) Lum, K.; Chandler, D.; Weeks, J. *J. Phys. Chem. B* **1999**, *103*, 4570.
(20) Reiss, H.; Frish, H.; Lebowitz, J. *J. Chem. Phys.* **1959**, *31*, 369.
(21) Reiss, H.; Frish, H.; Lebowitz, J. *J. Chem. Phys.* **1960**, *32*, 119.
(22) Pierotti, A. *Chem. Rev.* **1976**, *76*, 717.
(23) Cramer, C.; Truhlar, D. *Chem. Rev.* **1999**, *99*, 2161.
(24) Amovilli, C.; Barone, V.; Cammi, R.; Cancès, E.; Cossi, M.; Mennucci, B.; Pomelli, C. S.; Tomasi, J. *Adv. Quantum Chem.* **1999**, *32*, 227.
(25) Amovilli, C.; Floris, F. M. *Phys. Chem. Chem. Phys.* **2003**, *5*, 363.
(26) Nasehzadeh, A.; Azizi, K. *THEOCHEM* **2003**, *638*, 197.
(27) Floris, F. M. *J. Phys. Chem. B* **2004**, *108*, 16244.
(28) Rajamani, S.; Truskett, T. M.; Garde, S. *Proc. Natl. Acad. Sci. U.S.A.* **2005**, *102*, 9475.
(29) Ashbaugh, H. S.; Pratt, L. *Rev. Mod. Phys.* **2005**.

(30) Berendson, H.; Grigera, J.; Straatsma, T. *J. Phys. Chem.* **1987**, *91*, 6269.
(31) Boublik, T. *J. Chem. Phys.* **1970**, *53*, 471.
(32) Mansoori, G. A.; Carnhan, N. F.; Starling, K. E.; Leland, T. W. *J. Chem. Phys.* **1971**, *54*, 1523.
(33) Koenig, F. *J. Chem. Phys.* **1950**, *18*, 449.
(34) Hill, T. *J. Phys. Chem.* **1952**, *56*, 526−531.
(35) Buff, F. *J. Chem. Phys.* **1951**, *19*, 1591.
(36) Buff F. *J. Chem. Phys.* **1956**, *25*, 146−153.
(37) Defay, R.; Prigogine, I. *Tension superficielle et adsorption*; Éditions Desoer: 21, rue Ste-Vèronique, Lièege, 1951.
(38) Rowlinson, J.; Widom, B. *Molecular Theory of Capillarity*; Clarendon Press: Oxford, 1951.
(39) Rowlinson, J. *J. Phys. Cond. Matter* **1994**, *6*, A1.
(40) Tolman, R. *J. Chem. Phys.* **1949**, *17*, 333.
(41) Stillinger, F. H. *J. Solution Chem.* **1973**, *141*, 197.
(42) Pratt, L.; Pohorille, A. A. *Proc. EBSA Workshop on Water-Biomolecular Interactions* **1992**, *43*, 261.
(43) Ashbaugh, H. S.; Paulaitis, M. E. *J. Am. Chem. Soc.* **2001**, *123*, 10721.
(44) Ashbaugh, H.; Kaler, E.; Paulaitis, M. *J. Am. Chem. Soc*. **1999**, *121*, 9243.
(45) Hummer, G.; Garde, S.; García, A.; Pohorille, A.; Pratt, L. *Proc. Natl. Acad. Sci. U.S.A.* **1996**, *93*, 8951.
(46) Hummer, G.; Garde, S.; García, A.; Paulilatis, M.; Pratt, L. *J. Phys. Chem. B* **1998**, *102*, 10469.
(47) Garde, S.; Hummer, G.; García, A.; Paulilatis, M.; Pratt, L. *Phys. Rev. Lett.* **1996**, *77*, 4966.
(48) Gomez, M.; Pratt, L.; Hummer, G.; Garde, S. *Phys. Rev. Lett.* **1996**, *77*, 4966.
(49) van Giessen, A. E.; Blokuis, E. M. *J. Chem. Phys.* **2002**, *116*, 302.
(50) Helfrich, W. Z. *Z. Naturforch. C* **1973**, *28c*, 693.
(51) Ben-Naim, A. *J. Chem. Phys.* **1985**, *82*, 4662.
(52) Rowlinson, J. *Pure Appl. Chem.* **1993**, *65*, 873.
(53) Debenedetti, P. G.; Reiss, H. *J. Chem. Phys.* **1998**, *108*, 5498.
(54) Stillinger, F. H.; Cotter, M. A. *J. Chem. Phys.* **1971**, *55*, 3449.
(55) Evans, R.; Henderson, J. R.; Roth, R. *J. Chem. Phys.* **2004**, *121*, 12074.
(56) Stewart, M. C.; Evans, R. *Phys. Rev. E* **2005**, *71*, 11602.
(57) Jorgensen, W. *BOSS*, version 3.5; Yale University Press: New Haven, CT, 1994.
(58) Lazaridis, T. *J. Phys. Chem. B* **1998**, *102*, 3531.
(59) Zhang, Y.; Scott, E.; Brooks, B. R.; Pastor, R. W. *J. Chem. Phys.* **1995**, *103*, 10252.
(60) Berendson, H.; Postma, J.; van Gunsteren, W.; Hermans, J. *Intermolecular Forces*; Pullmann, B., Ed.; Reidel: Dordrecht, The Netherlands, 1981.